Research Article

Rana I. Mahmood, Alaa Al-Taie, Aya M. Al-Rahim, Harraa S. Mohammed-Salih, Humam Abdulrahman Ibrahim, Salim Albukhaty*, Sabrean F. Jawad, Majid S. Jabir*, Mohamed M. Salem, and Mounir M. Bekhit

Biogenic synthesized selenium nanoparticles combined chitosan nanoparticles controlled lung cancer growth *via* ROS generation and mitochondrial damage pathway

https://doi.org/10.1515/ntrev-2025-0142
received May 10, 2024; accepted January 21, 2025

Abstract: The green synthesis approach has drawn a lot of interest as an environmentally friendly and sustainable acceptable means of producing a diverse range of nanoparticles (NPs). This piece described a rapid approach for synthesizing selenium nanoparticles (SeNPs) with grape seed extract. A biologically active composition of selenium-chitosan nanoparticles (Se-chitosan NPs) has been prepared and characterized using, ultraviolet–visible, scanning electron microscopy, transmission electron microscopy, and zeta potential and size distribution experiments. To study the anticancer activity of prepared NP cytotoxicity (3-(4,5-dimethylthiazol-2-yl)-2,5-diphenyltetrazolium bromide) assay of chitosan nanoparticles (Chito-NPs), SeNPs were tested on two cancer cell lines: A549 and normal cell line (HK-2). In addition to a series of morphological changes, induction of apoptosis, reactive oxygen species (ROS) generation, and mitochondrial membrane potential. The results showed that the synthesized NPs were spherical with 55.285 and 30.9 nm, for SeNPs and Se-chitosan NPs, respectively. In the A549 cell line, SeNPs and Se-chitosan NPs exhibited dose-dependent cytotoxicity, with an IC_{50} for Chito-NPs of 24.09 µg/mL, whereas for SeNPs it was 18.56 µg/mL. Conversely, normal cell lines (MCF-10) were not significantly cytotoxically affected by SeNPs and Se-chitosan NPs. Additionally, SeNP and Se-chitosan NP treatment resulted in increased ROS generation and caused mitochondrial dysfunction. Based on ROS-mediated pathways, the results demonstrated that Chito-NPs, SeNPs, and Se-chitosan NPs cause apoptosis and death in A549 cells. As nanotherapeutics, Chito-NPs, SeNPs, and Se-chitosan NPs appear to offer a great deal of unrealized potential based on these findings. Further investigation is warranted and clinically significant to elucidate the specific therapeutic potential and safety of these NPs when applied *in vivo*. In this work, we show that exposure to SeNPs, Chito-NPs, and Se-chitosan NPs alters the human lung cancer cell line A549's ROS route of signaling, thereby causing the induction of apoptosis.

Keywords: chitosan, selenium, nanocomposite, LDH, anticancer, ROS, MMP

*** Corresponding author: Salim Albukhaty,** Department of Chemistry, College of Science, University of Misan, Maysan, 62001, Iraq; Al-Manarah College for Medical Sciences, Maysan, 62001, Iraq,
e-mail: albukhaty.salim@uomisan.edu.iq, albukhaty.salim@uomanara.edu.iq
*** Corresponding author: Majid S. Jabir,** Department of Applied Sciences, University of Technology, Baghdad, 10066, Iraq,
e-mail: 100131@uotechnology.edu.iq
Rana I. Mahmood: Department of Biomedical Engineering, College of Engineering, Al-Nahrain University, Jadriya, Baghdad, Iraq,
e-mail: rana.i.mahmood@nahrainuniv.edu.iq
Alaa Al-Taie: Department of Biomedical Engineering, College of Engineering, Al-Nahrain University, Jadriya, Baghdad, Iraq,
e-mail: alaa.ayyed@nahrainuniv.edu.iq
Aya M. Al-Rahim: Department of Molecular and Medical Biotechnology, College of Biotechnology, Al-Nahrain University, Jadriya, Baghdad, Iraq,
e-mail: aya.alrahim@ced.nahrainuniv.edu.iq
Harraa S. Mohammed-Salih: Department of Orthodontics, College of Dentistry, University of Baghdad, Baghdad 10047, Iraq,
e-mail: dr.harraas.ms@gmail.com
Humam Abdulrahman Ibrahim: Cardiopulmonary Perfusion Unit, Cardiac Surgery Department, Iraqi Center for Cardiac Diseases, Medical City Complex, Baghdad, Iraq, e-mail: Humam.obaydi@gmail.com
Sabrean F. Jawad: Department of Pharmacy, Al-Mustaqbal University College, 51001, Hillah, Babylon, Iraq,
e-mail: sabrean.f.Jawaad@uomus.edu.iq
Mohamed M. Salem: College of Medicine, Huazhong University of Science and Technology, Wuhan, Hubei, China,
e-mail: medozcockney@gmail.com
Mounir M. Bekhit: Department of Pharmaceutics, College of Pharmacy, King Saud University, PO Box 2457, Riyadh, 11451, Saudi Arabia,
e-mail: mbekhet@ksu.edu.sa

Open Access. © 2025 the author(s), published by De Gruyter. This work is licensed under the Creative Commons Attribution 4.0 International License.

1 Introduction

Nanotechnology and nanostructured materials have aided in the creation of cutting-edge materials with uses in nanomedicine, a branch of medicine [1,2]. It entails the catalytic production of medicinal medicines in nanoparticle (NP) form, which has a small particle size and high surface area [3,4]. Diverse samples obtained from the microorganism extracts, such as bacterial resources, micro and macro green algae, and botanical extracts, are employed in the natural production of NPs [5]. These samples are used as naturally occurring capping and reducing agents in the synthesis of metal and metal NP oxides in an environmentally sustainable manner. In contrast to the biosynthesis of NPs using fungi, bacteria, algae, and actinomycetes, green-produced NPs utilizing plant extract are more affordable and environmentally friendly. Increased reaction kinetics is the main benefit of green synthesis employing plant extract. Although medicinal plant components such as seeds, stems, roots and leaves are used to produce metal oxide nanoparticles (NPs), fruits are usually used because of their high phytochemical content [6].

Chitosan is a polysaccharide that is linear and abundant in nature, derived by chitin's deacetylation; it has a unique set of functional properties due to many reactive groups that contain –OH and $–NH_2$ [7,8]. It is well hydrophilic, biocompatible, biodegradable, nontoxic, nonimmunogenic, and low-cost polymer. Hence, it is intensively used in food, biotechnology, pharmacy, and agriculture [9]. Chitosan nanoparticles' (Chito-NPs) advantages in drug delivery applications stem from their capacity to interact with other organic chemicals and go through enzymatic hydrolysis [10]. Many parameters can control the drug encapsulation and release the properties of Chito-NPs just liked molecular weight, size, potential of the surface, and stability [11]. Selenium (Se) is considered a necessary component for humans. It has two forms in nature: organic and inorganic selenium. The most common forms of inorganic selenium are sodium selenite and selenate which are usually used as components of dietary supplements [12]. Selenium nanoparticles (SeNPs) have a variety of shapes and sizes [13], the manufacture of drugs [14], analysis of DNA [15], nuclear magnetic resonance imaging [16], biosensors [17], environmental rehabilitation [18], pharmaceuticals [19], agricultural [20], commercial uses, and electronics [21]. Their small size and large surface area, SeNPs exhibit unique physical and chemical characteristics [22]. SeNPs have various purposes, especially in medicine, because of their therapeutic benefits, which include low toxicity, enhanced reactivity, minimal dosage requirements, and superior absorption when weighed against Se's other oxidation states, including Se^{6+} and Sa^{4+} [23]. SeNPs are preferred over other forms of Se for biological activities because of their elevated biological activity and minimal toxicity [24]. Both chemical and inorganic methods can be used to create NPs [24,25]. Over the past few decades, interest in inorganic NPs for biomedical applications has grown. The interest in nanotoxicology, however, has grown over the past several years, and more information about the cytotoxic characteristics of inorganic NPs has been released [26]. Both humans and animals can use the biogenic NPs with little concern [27]. Because the microorganisms degrade selenites and selenates to nano-selenium through a detoxifying process, for the creation of distinct SeNPs, they are known as prospective biofactories [28]. Nada *et al.* produced SeNPs by using *Bacillus cereus* filtrate and increased its efficiency by gamma irradiation [29].

Chitosan and selenium together may improve the bioactivity, stability, and retention duration of selenium in the gastrointestinal tract. The primary determinants of the physicochemical characteristics of chitosan-based selenium composites are the chitosan's molecular weight, concentration, and functional groups, as well as the conditions of manufacture. Additionally, it demonstrated the potential of chitosan-based selenium composites as Se supplements to improve the nutritional value of crops and animals for human consumption, as well as their hepatoprotective, antibacterial, anti-diabetic, and anticancer qualities [30]. Polyphenolic chemicals and secondary metabolites, which are abundant in grape seed extract (GSE), exhibit strong bactericidal qualities that work against both Gram-positive and Gram-negative bacteria as well as other infections [31]. The extract's content, the proportion of phenols, and the kind of bacteria determine how well GSE inhibition works [32]. Additionally, GSE was examined for potential pharmacological and medically significant antioxidant, chemopreventive, cardioprotective, anti-inflammatory, and anticarcinogenic qualities [33]. In the end, non-biogenic methods render the NPs unfit for biomedical and dietary applications, whereas biogenic methods are secure, affordable, environmentally friendly, and nontoxic [34–36]. Using the human lung cancer cell line A549, we show in this research that exposure to SeNPs, Chito-NPs, and selenium nanoparticles combined chitosan nanoparticles (Se-chitosan NPs) modulates the reactive oxygen species (ROS) signaling pathway, which triggers the production of apoptosis.

2 Material and methods

2.1 Grape seed collection and preparation

The grape seeds were collected from Duhok City, Iraq. They were dried in the shade for 7–14 days and then ground into a fine powder using an electric mixer, followed by manual grinding. The active compounds are extracted by dispersing the powder (10 g) in deionized water (400 mL) for 150 min at 100°C. After obtaining a color solution, Whatman filter paper is used followed by centrifugation for further purification. The solution is stored in the fridge. The extraction process was carried out based on the works [37,38].

2.2 Preparation of SeNPs

The preparatory work was completed in compliance with some modifications [39–41]. A magnetic stirrer set at 600 rpm was used for 30 min to dissolve 2 g of sodium selenite (Na_2SeO_3) in deionized water (100 mL). Following full dissolution, 300 mL of GSE was combined with the precursor solution and then utilized a magnetic stirrer to mix for an hour. Subsequently, 50 mL of 10% hydrochloric acid (HCL) was pipetted into the mixture until a reddish-orange coloration occurred and a precipitate formed. After being separated using a centrifuge, the precipitate is repeatedly cleaned using ethanol and water. The precipitate was dried for 4 h at 100°C in an oven.

2.3 Chito-NP and Se-chitosan NP preparation

A solution of 0.33 g of citric acid ($C_3H_2O_7$) was dissolving the acid in deionized water (50 mL) using a magnetic stirrer for 30 min. Subsequently, 0.5 g chitosan was stirred with the acidic solution until fully dissolved. In parallel, 0.085 g of SeNPs were dispersed by magnetic stirring with 11 mL of deionized water for 30 min. To synthesize the nanocomposite, 1.5 mL of the SeNP dispersion, after being stirred for 70 min at 100°C, was combined with 25 mL of the chitosan solution. The resulting nanocomposite exhibited a distinct viscosity and a characteristic blood-red color.

2.4 Characterization of SeNPs

2.4.1 Ultraviolet–visible (UV–Vis) spectroscopy, transmission electron microscopy (TEM), and scanning electron microscopy/energy-dispersive X-ray spectroscopy (SEM–EDX)

UV–Vis (Analytik-Jena AG, Germany) and TEM (BRUKER Alpha, Germany) techniques were used to describe the characteristics of the SeNPs, Chito-NPs, and Se-chitosan NPs. EDS coupled with SEM to get the elemental composition with the shape of SeNPs, Chito-NPs, and Se-chitosan NPs. By using ultraviolet light and laminar airflow, the samples were sterilized. Following disinfection, the NPs were evenly carbon coated (JEOL-EC-32010CC) and used adhesive tape for carefully positioned on SEM stubs. They were then put in a sample chamber of SEM-EDS (JEOL JSM-IT 100, Japan) and scanned at various magnifications, ranging from 6,000 to 8,000 while being subjected to a voltage of 20 kV.

2.4.2 Particle size and zeta potential (ZP)

Zetasizer Nano Series (Malvern Version 7.02, Malvern Instruments Ltd., UK) was used to conduct ZP and size distribution experiments. To ascertain the ZP and particle size distribution, after dissolving the ingredients in deionized water, they were sonicated for 8 min. The dip cell kit's cuvette was then filled with just over 0.5 mL of the fluid.

2.5 Cells and reagents

Lung cancer epithelial cells (A549 cells) and normal cells (MCF-10 cells) were purchased from (Sigma) (KPL). RPMI-1640, 3-(4,5-dimethylthiazol-2-yl)-2,5-diphenyltetrazolium bromide (MTT), fetal bovine serum, dimethyl sulfoxide (DMSO), trypsin–EDTA (Capricorn Scientific GmbH, Ebsdorfergrund, Germany), and Triton X-100 were all acquired from Sigma.

2.6 Cell lines culturing

PRMI-1640 (Sigma, USA) medium (Capricorn Scientific GmbH) containing 10% fetal bovine serum, 100 units/mL penicillin, and 100 g/mL streptomycin was used to culture A549 and MCF-10 cell lines. Trypsin–EDTA trypsinizes adherent monolayers that were cultivated at 37°C in an incubator with 5% CO_2 for a short time. These cells undergo regular verification and testing.

2.7 Cytotoxicity assay

The MTT protocol was employed for cytotoxicity examination of the Chito-NPs, SeNPs, and Se-chitosan NPs. A549 and a density of 1×10^4 MCF-10 cells per well were used to seed the cells into 96-well plates following an overnight culture. Following removing the growing medium and adding 200 µL of fresh medium with varying doses of SeNPs, Chito-NPs, and Se-chitosan NPs (12.5–200 µg/mL) for 72 h [42–44]. Following a 3-h wash with tepid water, the cells were stained with 3-(4,5-dimethylthiazol-2-yl)-2,5-diphenyltetrazolium bromide (MTT) solution at a concentration of 2 mg/mL (Invitrogen, Carlsbad, CA). Each well had its solution drained off before 100 µL of DMSO was added. A microplate reader was used to measure each sample's absorbance at a wavelength of 492 nm [45,46]. The formula determined the rate at which cell growth was inhibited, or the cytotoxicity percentage:

$$\text{Cytotoxicity } \% = \frac{A - B}{A},$$

where A represents the sample's optical density while B is the control's optical density [47].

2.8 Lactate dehydrogenase (LDH) release assay

This assay was carried out in compliance with the guidelines provided by the manufacturer for assessing toxicity in cultured cell lines. The cells were treated with Chito-NPs, SeNPs, and selenium-chitosan NPs for 24, 48, and 72 h. A 96-well plate was filled with the treated cells' supernatant so that optical density at 490 nm could be used to evaluate LDH release characteristics [48].

2.9 Flow cytometry assay

A test of flow cytometry was used to quantify ROS amount produced by cells. A total of 10^6 of A549 cells seeded per well. The cells were treated with Chito-NPs, SeNPs, and Se-chitosan NPs for 10 h after being incubated for the entire night at IC_{50} concentrations of 24.09 and 18.56 µg/mL, respectively. Next, a 20 µM concentration of DCFH-DA ROS probe (Cat No. 35845, Sigma) was added to the fresh medium, and it incubated in the dark for an additional 30 min. A flow cytometer quantified the cells' fluorescence intensity. Moreover, following treatment with Chito-NPs, SeNPs, and Se-chitosan NPs, lung cell line treatment was utilized to measure mitochondrial membrane potential (MMP) using a Rhodamine probe (Cat No. 83695, Sigma). The intensity of each cell's fluorescence was measured by a flow cytometer and CyAn ADP (Beckman Coulter, CY20030) following pre-established procedures.

2.10 Acridine orange/ethidium bromide (AO/EtBr) staining

The A549 cells were plated in 12-well plates after being harvested. After being incubated for 24 h, the cells were exposed to Se-NPs, Se-chitosan NPs, and Chito-NPs for 24 h. After that, the cells were dyed for 2 min at 37°C with 10 µg/mL AO/EtBr so that the fluorescent microscope could detect them.

2.11 Apoptosis detection Annexin V/PI assay

Following treatment with Chito-NPs, SeNPs, and Se-chitosan NPs, the current study examined apoptosis in A549 lung cancer cells. The cells were gathered after a day and given two cold phosphate-buffered solution washes. After that, the cells were stained for 30 min using PI and Annexin V FITC. The labeled cells were examined using flow cytometry, which made it possible to determine whether apoptosis had occurred.

2.12 Statistical analysis

The information that is being displayed is based on three separate experiments. A mean and a standard deviation were used to represent the data. The significance of the differences was assessed using the two-tailed Student's t-test. For the statistical analysis, GraphPad Prism was used (USA). A statistically significant result was obtained when $p < 0.05$ [44,49].

3 Results and discussion

3.1 Characterization

Successful NP production is shown by UV–Vis spectroscopy characterization. The UV–Vis method is one of the most important ways to ascertain whether the formation of NPs signifies the existence of metal surface plasmon resonance (SPR). The reaction solution was scanned between 300 and 800 nm in wavelength. Although there is no peak for Chito-NPs in the UV–Vis absorption spectrum, Figure 1 shows a noticeable peak at $\lambda_{max} \sim 305$ nm and $\lambda_{max} \sim 290$ nm, respectively, which establishes this formed material's SPR has been induced Chito-NPs and SeNPs. The prepared NPs were shown in spherical forms, as shown in Figure 2, and were validated by TEM. The results of SEM images are shown in Figures 3–5(a). The SEM electron microscope offers great resolution at a low voltage so it is a good tool for imaging NPs. As has been documented in multiple investigations, the spherical and uniform shape of the produced SeNPs may be observed using the SEM technique [50,51]. The EDX analysis of SeNPs and Se-chitosan NPs exhibited that absorption peaks were the same (1.4), as shown in Figures 4 and 5(b). Using an electron microscope to scan the component elements, EDX analysis identifies their composition and concentrations [52,53]. Observed in the elemental analysis of free SeNPs and combined Se-chitosan NPs, reflected that absorption peaks were 1.4. The selenium element in the free SeNPs was associated with the highest peak. In various investigations, such as Fernández-Llamosas *et al.* [54], Srivastava and Mukhopadhyay [55], Cremonini *et al.* [56], Sharma *et al.* [57], and Dhanjal and Cameotra [58], the greatest peak associated with selenium production, found at 1.4, was investigated. The produced NPs' spherical forms, as shown in Figure 4, were validated by TEM data.

The produced NPs were spherical and had average sizes of 55.285 and 30.9 nm for SeNPs and Se-chitosan NPs, respectively. As shown in Table 1. The ZP of synthesized Chito-NPs, SeNPs, and Se-chitosan NPs is shown in Figures 6–8. NP's ZP has been observed at varying rates in earlier research. For example, −7.7 mV was detected by Srivastava and Mukhopadhyay [59] and −28.8 mV was documented by Vekariya *et al.* [60]. In another study, the ZP was found to be −22.9 mV for synthetic SeNPs using fungus was −22.9 mV [61].

3.2 Chito-NPs, SeNPs, and Se-chitosan NPs increase the LDH release

The enzyme LDH regulates the process by which lactate is converted to pyruvate, a process that needs cellular energy. LDH was used to evaluate the cytotoxic effects of Chito-NPs, SeNPs, and Se-chitosan NPs on lung cancer cell lines. Damage to the A549 cells subjected to Chito-NPs, SeNPs, and Se-

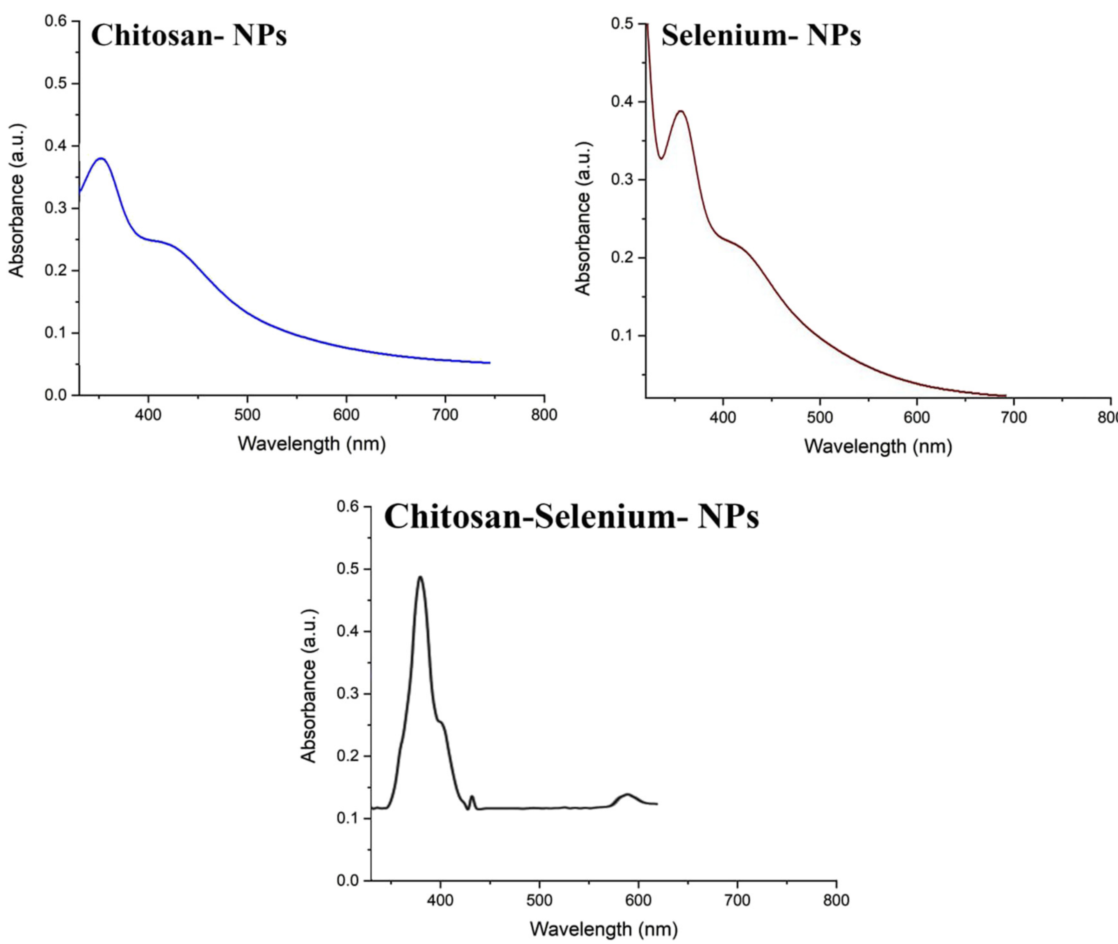

Figure 1: UV–Vis spectra of prepared NPs.

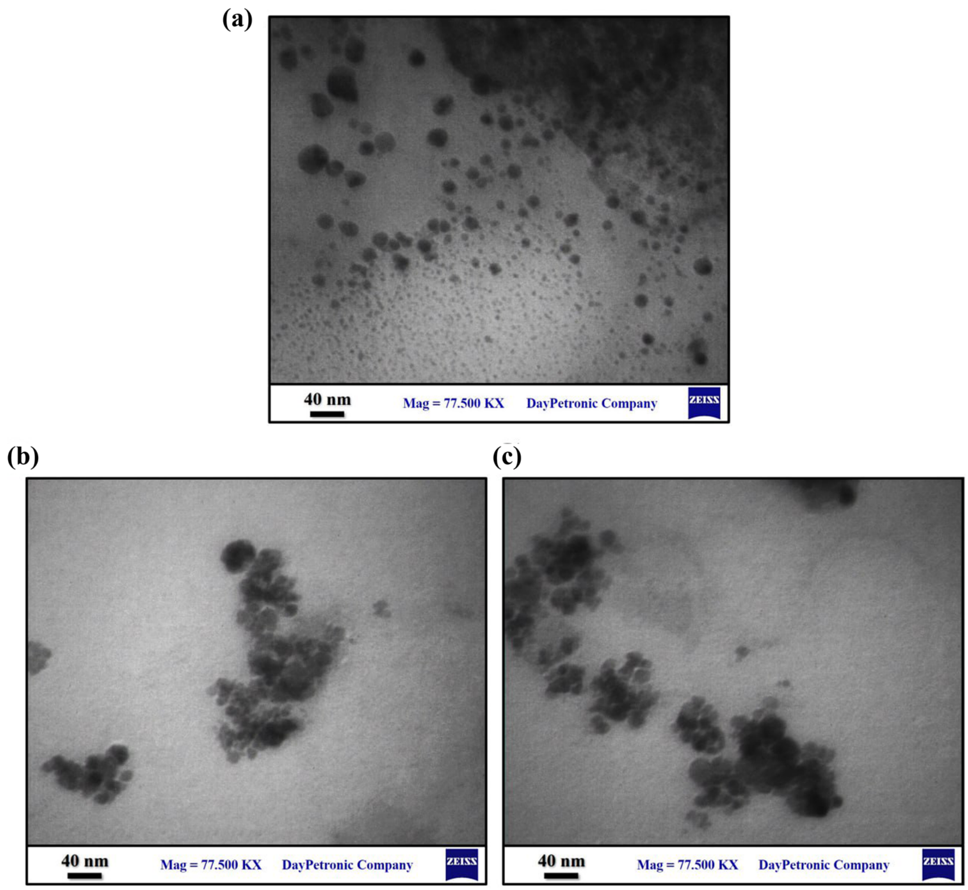

Figure 2: TEM images of chitosan NPs (a), SeNPs (b), and Se-chitosan NPs (c).

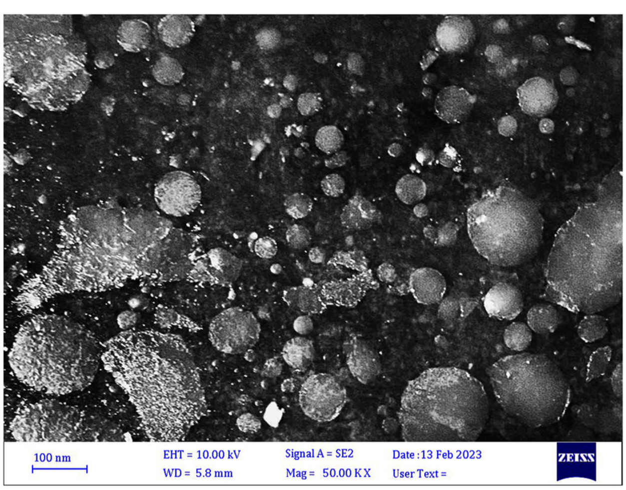

Figure 3: SEM–EDX of Chito-NPs.

chitosan NPs produces formazan from tetrazolium salt by releasing LDH from the cytoplasm. After lung cancer cells are handled with Chito-NPs, SeNPs, and Se-chitosan NPs, the proportion of released LDH in the suffering or dying cells is ascertained through measurement of the creation of formazan at a wavelength of 490 nm. The generation of formazan at a wavelength of 490 nm is measured to determine the percentage of LDH released in a lung carcinoma that is sick or dying. The information gathered suggests that Chito-NPs, SeNPs, and Se-chitosan NPs may be able to penetrate treated cells and induce vesicle development. The effect of concentration on the potential for LDH release by SeNPs, Chito-NPs, and Se-chitosan NPs is shown in Figure 9. The ability of Chito-NPs, SeNPs, and Se-chitosan NPs to enter cells as well as additional biological elements can lead to significant cellular disruption and induce the release of LDH. Concurrently, cells may absorb 100–200 nm NPs, which may trigger deleterious effects including genetic material mutations or DNA damage. The toxicity of NPs is probably related to processes that, by interfering with the antioxidant system, increase the body's oxidative stress level [62]. Numerous membranes, such as those enclosing the mitochondria and the cell, have been damaged, which is caused by free radicals such as ROS. Because of this, the elements of cells that cause cell death, including proteins, lipids, fatty acids, and nucleic

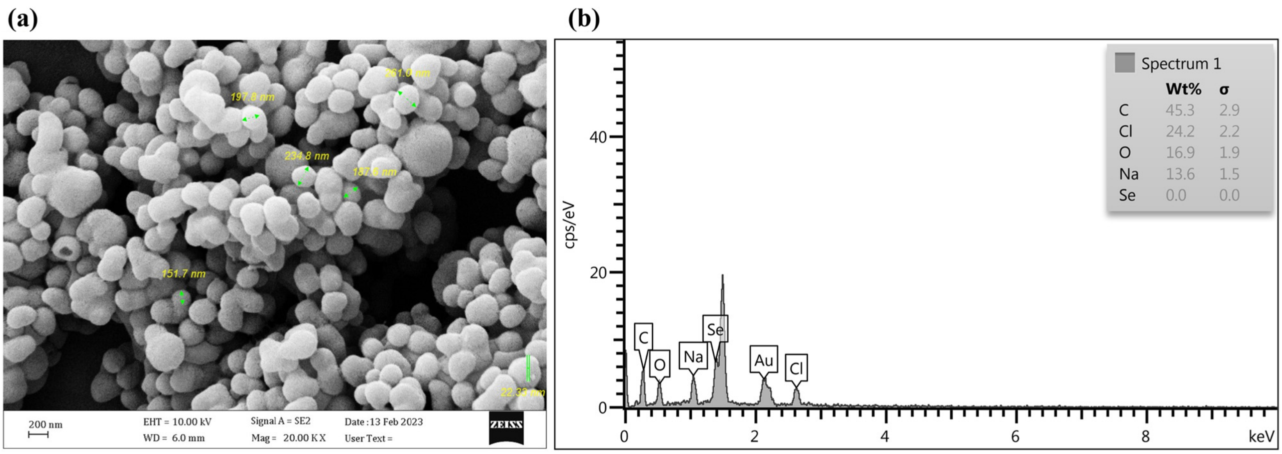

Figure 4: SEM–EDX of SeNPs. (a) SEM micrographs of SeNPs. (b) EDX analysis of SeNPs. SEM, scanning electron microscopy; EDX, energy-dispersive X-ray spectroscopy.

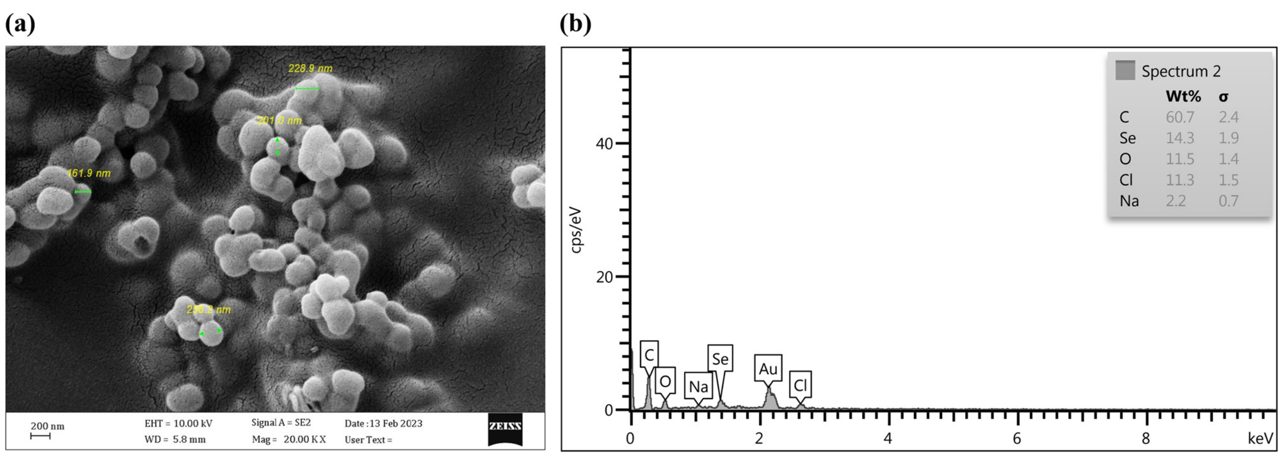

Figure 5: SEM–EDX of Se-chitosan NPs. (a) SEM micrographs of Se-chitosan NPs. (b) EDX analysis of Se-chitosan NPs. SEM, scanning electron microscopy; EDX, energy-dispersive X-ray spectroscopy.

Table 1: SeNPs and Se-chitosan NPs sizes and ZP. Three different experiments' worth of data are presented in triplicate as ± standard deviation means

Particles	Size (nm)	ZP (mV)
SeNPs	55.285	−15.4 ± 3.94
Se-chitosan NPs	30.9	13.8 ± 3.22

acids, interfere with the process of electronic information transfer. The cytotoxicity of A549 cells could perhaps be attributed to oxidative stress, which results in cellular disintegration. Furthermore, Chito-NPs, SeNPs, and Se-chitosan NPs may trigger concentration-dependent release of LDH, which could be related to cell membrane injury. The breakdown of cellular membranes, which releases cellular enzymes like LDH into the surrounding environment, could be connected to the LDH release that occurs in response to concentration-dependently to Chito-NPs, SeNPs, and Se-chitosan NPs.

3.3 Anticancer activity of NPs against lung cancer cells

Following a 72-h therapy course at different quantities of Chito-NPs, SeNPs, and Se-chitosan NPs (12.5, 25, 50, 100, and 200 g/mL), Chito-NPs, SeNPs, and Se-chitosan NPs were tested on lung cancer cells to see if they might stop growth suppression and proliferation. Chito-NPs, SeNPs, and Se-chitosan NPs reduced the cell viability that was dependent on dose, as cleared in Figure 10 (left panel). The inhibitory

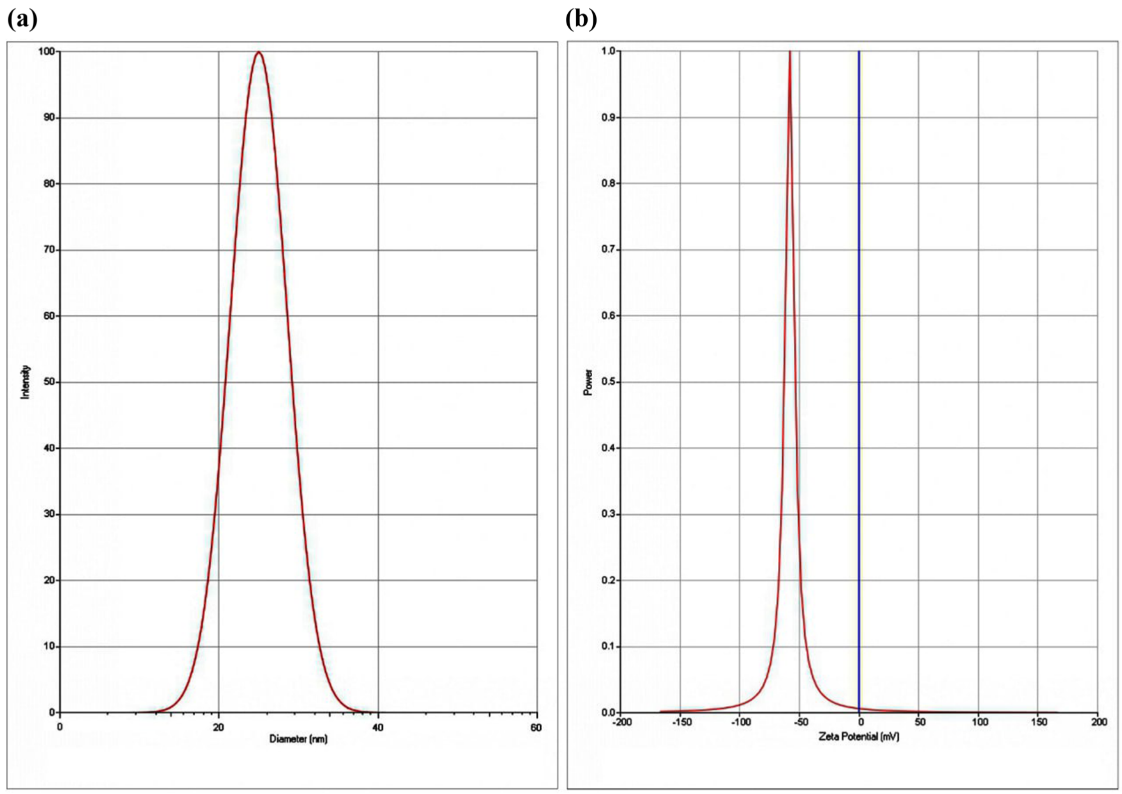

Figure 6: (a) Particle size distribution and (b) Chito-NPs' ZP.

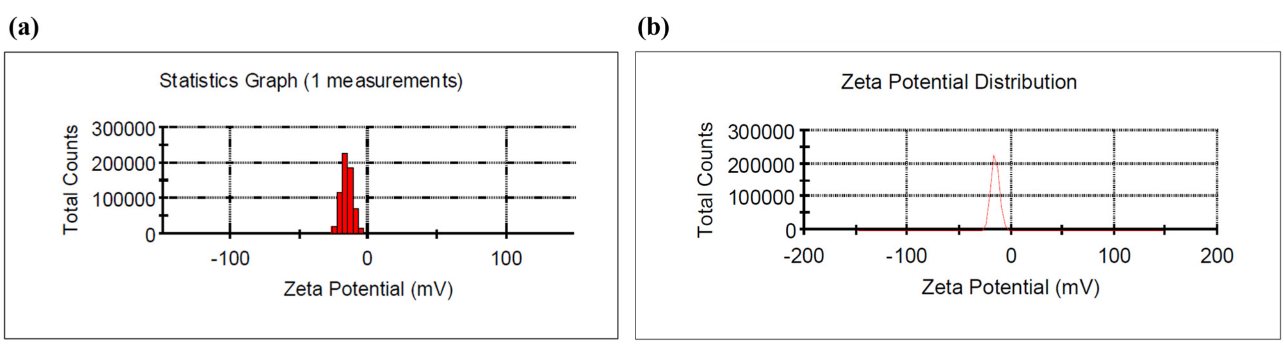

Figure 7: (a) Particle size distribution and (b) SeNPs' ZP.

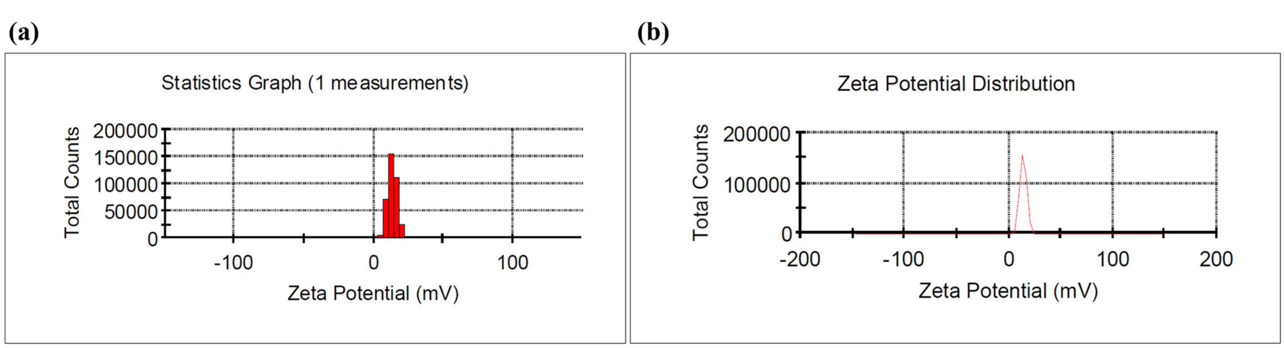

Figure 8: (a) Particle size distribution and (b) Se-chitosan NPs ZP.

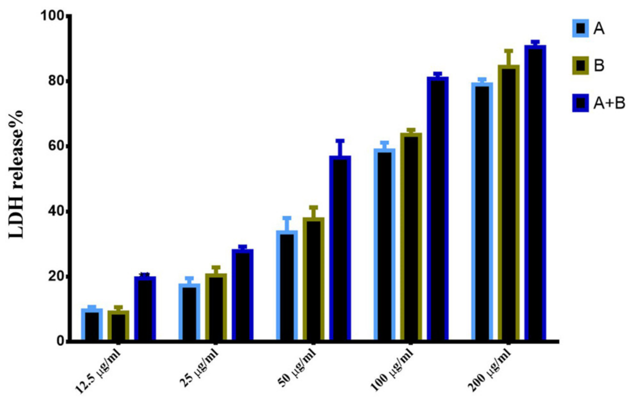

Figure 9: Prepared NPs induce LDH release in lung cancer cells. A = Chito-NPs, B = SeNPs, and A + B = Se-chitosan NPs.

concentration (IC_{50}) for Chito-NPs was at a quantity of 24.09 µg/mL, whereas the quantity for SeNPs was 18.56 µg/mL following a 72 h treatment with high quantities of Se-chitosan NPs, the viability of A549 cells decreased to almost 10%. This study's findings indicated that the Chito-NPs and SeNPs caused cell death, and this inhibitory effect was improved by combining these two NPs as showed in the Se-chitosan NPs treated cells. In addition, acridine orange and ethidium bromide were used in a dual staining technique to analyze the nuclear morphology of the treated cells. The criterion for classifying apoptotic cells was DNA damage. Within the framework of this investigation, a look was also taken at how effective the Chito-NPs, SeNPs, and Se-chitosan NPs. To examine the different apoptotic features of the nuclear alterations, AO-EB staining was used. Following AO-EtBr staining, non-apoptotic cells displayed a green tone, while apoptotic cells displayed an orange or red coloration. As indicated in Figure 10 (right panel), there were significantly more apoptotic cells in the cells treated with Chito-NPs, SeNPs, and Se-chitosan NPs than in the untreated cells. These results were consistent with earlier research showing that Chito-NPs and SeNPs both exhibited apoptotic properties. According to a published study, SeNPs activated Ca^{2+} signals in various cancer cell lines. The stimulation of the process of apoptosis in cancer cell lines can be determined by their varying susceptibility to SeNPs. This can be achieved by processes of ER stress, modulation of the Ca^{2+} signaling system, and the initiation of several gene expression patterns that code for pro-apoptotic proteins [63]. Another investigation found that applying SeNPs to colon cancer cell lines caused immunogenic cell death is indicated by pro-apoptotic and immunogenic cell death markers. It also showed that these NPs could be an effective way to kill tumor cells indirectly by enhancing immunogenicity and causing apoptosis [64]. Also, according to a study, the combination of radiation and nano-Se inhibits the multiplication of lung cancer cells, hence acting as an anticancer agent [65]. Likewise, Shen and colleagues found that chitosan oligosaccharide (COS) *in vitro* reduced the quantity of S phase cells, inhibited cell proliferation, and slowed down the DNA synthesis rate due to an increase in p21 with cyclin A

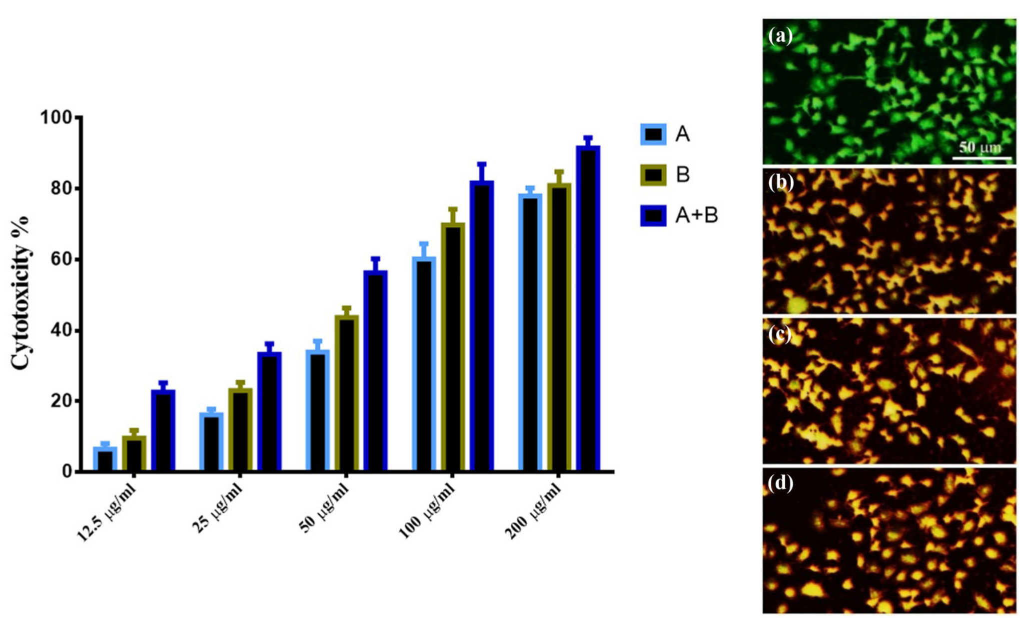

Figure 10: Anti-proliferative activity of prepared NPs against lung cancer cells. The right panel represented the cytotoxicity of prepared NPs against lung cancer cells. A = Chito-NPs, B = SeNPs, and A + B = Se-chitosan NPs. The left panel represented AO/EtBr double staining assay. A = control untreated cells, B = Chito-NPs, C = SeNPs, and D = Se-chitosan NPs.

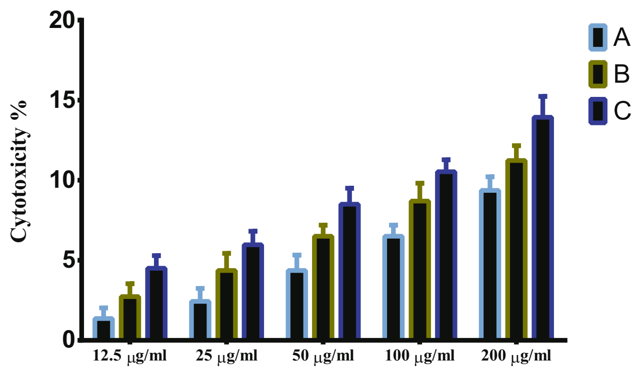

Figure 11: Anti-proliferative activity of prepared NPs against normal breast cell line (MCF-10). A = Chito-NPs, B = SeNPs, and A + B = Se-chitosan NPs.

and CDK-2 decrease. COS impeded the growth of tumors by inhibiting the metastatic associated protein (MMP-9) in Lewis lung carcinoma (LLC) cells [66]. It may be possible to enhance the anticancer and nanotherapeutic effects of Chito-NPs on various human cancer cell lines [67]. On the other hand, the results showed a low cytotoxic effect against normal cell lines as indicated in Figure 11.

According to the flow cytometry data, the cells in quadrant Q3 that were going through apoptosis had Annexin V labels on them. Dot plots of A549 cells treated with SeNPs, Chito-NPs, and Se-chitosan NPs for 24 h at an IC_{50} concentration are displayed in Figure 12. While the majority of cells in the control A549 (97.5%) were viable and not undergoing apoptosis, the A549 treated with Chito-NPs, SeNPs, and Se-chitosan NPs showed a rise in apoptotic cells and a fall in viable cells. In the A549 control group, 0.56% of the cells were apoptotic. In contrast, the proportion rose to 86.5, 90.3, and 95.1% in A549 cells administered with Chito-NPs, SeNPs, and Se-chitosan NPs, respectively. Furthermore, the study's findings have shown that Chito-NPs, SeNPs, and Se-chitosan NPs have no harmful effects on the typical cell line of the human lung, as clear in Figure 11. There are multiple possible ways that carbon nanotubes (CNTs) could damage lung cancer cells. One explanation for this is that they function as oxidative triggers, which encourage DNA damage and inflammation [68]. Our study's findings demonstrated that the viability of A549 cells was considerably decreased when they were treated with Chito-NPs, SeNPs, and Se-chitosan NPs. Large quantities of ZnO-Fe_3O_4 composite magnetic NPs were shown to be fatal for the human cell line for breast cancer MDA-MB-231, but that is not for typical mouse fibroblasts (NIH 3T3), according to research by Bisht *et al.* [69]. The typical mouse fibroblast does not exhibit this impact. According to a prior study, metal NP cytotoxicity may be brought on by the generation of free radicals and oxygen species that are reactive (ROS) [70]. It has also been observed that elevated ROS levels can cause apoptosis by activating FOXO3a, a protein that can improve apoptosis signaling by encouraging the production of pro-apoptotic mitochondria-targeting protein members of the Bcl2 family [71]. The idea that high ROS can trigger apoptosis is supported by this finding. This finding was made possible by the activation of FOXO3a, which happens when ROS levels are too high. According to the ROS assay results, the presence of ZnO/CNT@Fe3O4 significantly increased the K562 cell line's ROS generation amount. Observing these outcomes was interesting. Notably, current studies have shown that blocking the pathway of NF-kB with bortezomib, a well-known proteasome inhibitor increased the susceptibility of K562 cells to the deadly effects of ZnO/CNT@Fe3O4. This finding supports a theory that ZnO/CNT@Fe_3O_4-induced reduction of K562 cell sensitivity is most likely caused by nuclear factor-B pathway activation.

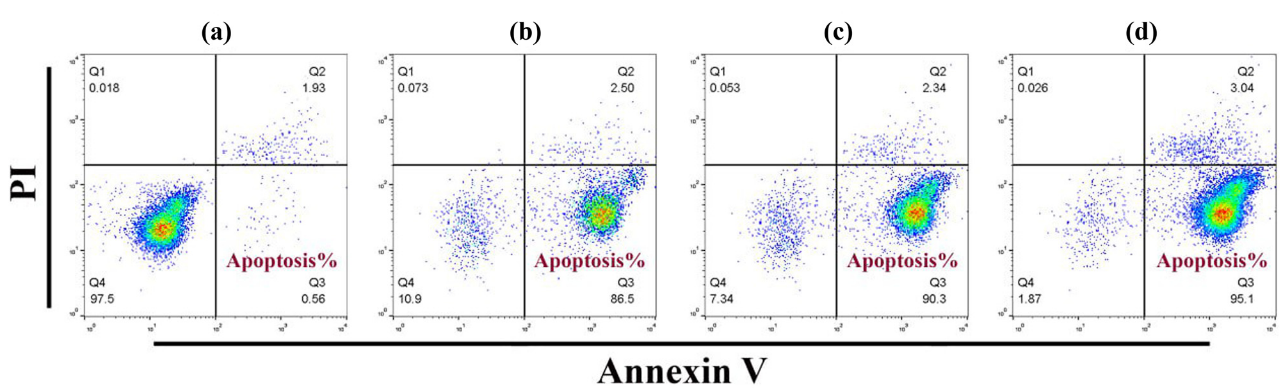

Figure 12: Prepared NPs induce apoptosis in A549 cells using Annexin V assay. a = control cells, b = Chito-NPs, c = SeNPs, and d = Se-chitosan NPs.

3.4 Chito-NPs, SeNPs, and Se-chitosan NPs disorder oxidative balance in A549 cells

Cells treated with SeNPs, Chito-NPs, and Se-chitosan NPs showed a significant increase in ROS production. Compared to the control cells, the ROS-induced fluorescence signal was observed to be higher. The current work examined the accumulation of ROS within cell lines of lung cancer following counseling by Chito-NPs, SeNPs, and Se-chitosan NPs. After treatment with Chito-NPs, SeNPs, and Se-chitosan NPs, there was a noticeable rise in ROS in the cells. A DCFH-DA probe was used to measure the levels of ROS, as illustrated in Figure 13 (upper panel). The level of ROS was increased in the lung cancer cells after treatment with Chito-NPs, SeNPs, and Se-chitosan NPs [72]. We looked at the potential effects of therapy with Chito-NPs, SeNPs, and Se-chitosan NPs on mitochondrial function. The presence of rhodamine dye, which shows current-dependent accumulation in the mitochondria, allowed for the detection of the loss of the MMP. The results of this study showed, as shown in Figure 13 (lower panel), that after exposure to Chito-NPs, SeNPs, and Se-chitosan NPs at dosages IC_{50} for 24 h, The proportion of cells with a depolarized mitochondrial membrane rose dramatically, and the effect of Se-chitosan NPs was the highest among all groups. Selenium is contained in the selenoproteins and seleno-enzymes structure, which can inhibit ROS and, as a result, oxidative damage development [73]. The majority of the pharmaceutical components that are currently available come from natural products. Despite advancements, creating bioactive molecules and medications from natural products has proven difficult, partly due to the issue of large-scale sequestration and mechanistic comprehension. As the field of cancer, treatment has advanced significantly and the usage of advanced technology has increased [74]. The cytoskeleton, cell growth and proliferation, the cell cycle, inflammation, angiogenesis, cell signaling, intrinsic apoptosis, and reducing chemoresistance are among the multitargeted functions of phenolics. Because the normal ovarian cell lineage can handle phenolic acids well, they are effective prophylactic agents against ovarian cancer. However, cancer treatment may benefit from the nonflavonoids' antioxidant properties [75]. In recently published study [76], successfully created lipid nanocarriers using materials that the USFDA has designated as generally recognized as safe to address drug-related issues. This study aimed to assess the therapeutic efficacy of 6-*o*-stearoyl ascorbic acid nanostructured lipid carriers applied to CRT against mice suffering from colitis produced by dextran sodium sulphate. In addition to inhibiting the production of ROS during hypoxia and schemia/reoxygenation, selenium compounds stimulate mitochondrial biogenesis, which raises within-cell ATP and Ca^{2+} equilibrium levels with increased persistence of cells in the zone of penumbra [77,78]. The biogenic

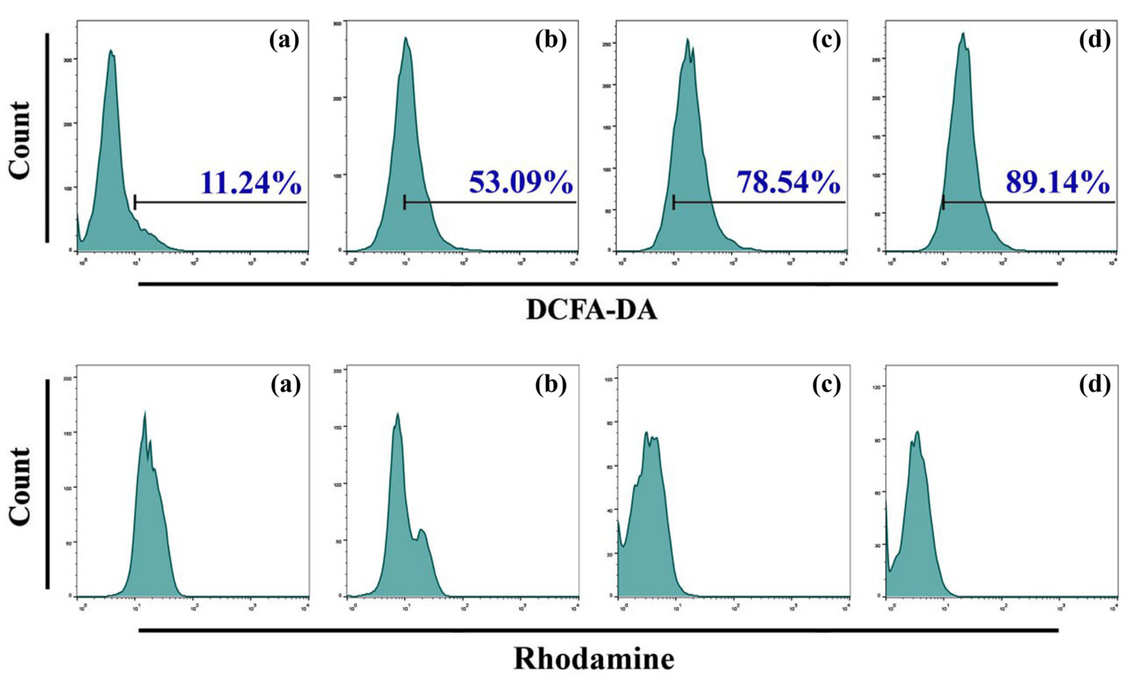

Figure 13: Chito-NPs, SeNPs, and Se-chitosan NPs cause mitochondrial malfunction and the production of ROS in A549 cells. (a) Untreated cells in control. (b) Cells subjected to Chito-NPs. (c) Cells exposed to SeNPs. (d) Cells treated to Se-chitosan NPs.

MgO NPs demonstrated their therapeutic potential against MDA-MB-231 cells by increasing cytotoxicity, inducing apoptosis, enhancing ROS production, promoting cell adhesion, and inhibiting cellular migration in a dose-dependent manner [79]. The results by Alserihi *et al.* [80] show that EGCG and EGCG NPs are effective anticancer agents in 3D spheroids of PCa cell lines. Following treatment with EGCG and EGCG NPs, the spheroid diameters of the cell lines under study were considerably decreased. EGCG and EGCG NPs caused ROS in PC3 cells but not in 22Rv1 cells, which may indicate that receptor-mediated antigens like PSMA are not involved. The MMP in 22Rv1 and PC3 spheroids treated with EGCG or EGCG NP did not significantly change. SeNPs have both prooxidant and antioxidant qualities, depending on the dosage. It has been demonstrated that a 12 μM concentration of SeNPs increases the cells' antioxidant capacity, while a 24 μM concentration of SeNPs decreases the cells' antioxidant capacity [81]. SeNPs induce ROS overproduction inside cancerous cells because of the acidic condition of pH and the imbalance of redox, which compromises mitochondrial integrity and causes ER stress. Numerous biochemical pathways, including NFκB, MAPK/Erk, Wnt/βcatenin, PI3K/Akt/mTOR, and the pathways of apoptotic, are activated as a result, leading to cellular stress [82].

4 Conclusions

The pharmacological potential of SeNPs and Chito-NPs is well known, and its nanoformulation is expected to have major therapeutic benefits, especially in the fight against cancer. In this work, we examined the anticancer potential of SeNPs and Se-chitosan NPs that were biogenically produced against lung cancer cells (A549). Many biological assessments were estimated, including cytotoxicity, cellular morphology, apoptosis induction, ROS generation, and MMP. The biogenic NPs demonstrated their therapeutic potential against A549 cells by increasing cytotoxicity, inducing apoptosis, and enhancing ROS generation and mitochondrial dysfunction. The outcomes of the *in vitro* experiments cleared the ROS-mediated pathways used by Chito-NPs, SeNPs, and Se-chitosan NPs to trigger death in A549 cells. These results also imply that a lot of promise remains untapped. Further investigation is warranted and clinically significant to clarify a safety with comprehensive of the potential therapeutic of these NPs once applied *in vivo*. In the current work, we establish that exposing cells to SeNPs, Chito-NPs, and Se-chitosan NPs alters the human lung cancer cell line A549's ROS signaling pathway, causing the induction of apoptosis. The given results may contribute to the creation of more potent medications for the treatment of lung cancer in humans.

Acknowledgments: The authors enjoy feeling their profound gratitude to the University of Technology-Iraq. The authors would like to extend their sincere appreciation to the Researchers Supporting Project Number (RSPD2025R986), King Saud University, Riyadh, Saudi Arabia.

Funding information: The authors state no funding involved.

Author contributions: All authors have accepted responsibility for the entire content of this manuscript and approved its submission.

Conflict of interest: The authors state no conflict of interest.

Data availability statement: All data generated or analyzed during this study are included in this published article.

References

[1] Tabrez S, Khan AU, Mirza AA, Suhail M, Jabir NR, Zughaibi TA, et al. Biosynthesis of copper oxide nanoparticles and its therapeutic efficacy against colon cancer. Nanotechnol Rev. 2022 Mar;11(1):1322–31.

[2] Tabrez S, Khan AU, Hoque M, Suhail M, Khan MI, Zughaibi TA. Investigating the anticancer efficacy of biogenic synthesized MgONPs: An in vitro analysis. Front Chem. 2022 Sep;10:970193.

[3] Gowd V, Ahmad A, Tarique M, Suhail M, Zughaibi TA, Tabrez S, et al. Advancement of cancer immunotherapy using nanoparticles-based nanomedicine. Semin Cancer Biol. 2022;S1044-579X(22)00081-5. doi: 10.1016/j.semcancer.2022.03.026.

[4] Alserihi RF, Mohammed MR, Kaleem M, Khan MI, Sechi M, Sanna V, et al. Development of (−)-epigallocatechin-3-gallate-loaded folate receptor-targeted nanoparticles for prostate cancer treatment. Nanotechnol Rev. 2021 Dec;11(1):298–311.

[5] Alafaleq NO, Zughaibi TA, Jabir NR, Khan AU, Khan MS, Tabrez S. Biogenic synthesis of Cu-Mn bimetallic nanoparticles using pumpkin seeds extract and their characterization and anticancer efficacy. Nanomaterials. 2023 Mar;13(7):1201.

[6] Kadhim AA, Abbas NR, Kadhum HH, Albukhaty S, Jabir MS, Naji AM, et al. Investigating the effects of biogenic zinc oxide nanoparticles produced using papaver somniferum extract on oxidative stress, cytotoxicity, and the induction of apoptosis in the THP-1 cell line. Biol Trace Elem Res. 2023;201(10):4697–709.

[7] Chen W, Yue L, Jiang Q, Liu X, Xia W. Synthesis of varisized chitosan-selenium nanocomposites through heating treatment and evaluation of their antioxidant properties. Int J Biol macromolecules. 2018 Jul;114:751–8.

[8] Kołodyńska D, Hałas P, Franus M, Hubicki Z. Zeolite properties improvement by chitosan modification – Sorption studies. J Ind Eng Chem. 2017 Aug;52:187–96.

[9] Salar S, Mehrnejad F, Sajedi RH, Arough JM. Chitosan nanoparticles-trypsin interactions: Bio-physicochemical and molecular dynamics simulation studies. Int J Biol Macromolecules. 2017 Oct;103:902–9.
[10] Cao H, Xiao J, Liu H. Enhanced oxidase-like activity of selenium nanoparticles stabilized by chitosan and application in a facile colorimetric assay for mercury (II). Biochem Eng J. 2019 Dec;152:107384.
[11] Song X, Chen Y, Zhao G, Sun H, Che H, Leng X. Effect of molecular weight of chitosan and its oligosaccharides on antitumor activities of chitosan-selenium nanoparticles. Carbohydr Polym. 2020 Mar;231:115689.
[12] Rayman MP. Selenium and human health. Lancet. 2012;379(9822):1256–68.
[13] Sharma A, Goyal AK, Rath G. Recent advances in metal nanoparticles in cancer therapy. J Drug Target. 2018 Sep;26(8):617–32.
[14] Adeyemi OS, Sulaiman FA. Evaluation of metal nanoparticles for drug delivery systems. J Biomed Res. 2014 Dec;29(2):145.
[15] Kwon SJ, Bard AJ. DNA analysis by application of Pt nanoparticle electrochemical amplification with single label response. J Am Chem Soc. 2012 Jul;134(26):10777–9.
[16] Sun C, Lee JS, Zhang M. Magnetic nanoparticles in MR imaging and drug delivery. Adv Drug Delivery Rev. 2008 Aug;60(11):1252–65.
[17] Doria G, Conde J, Veigas B, Giestas L, Almeida C, Assunção M, et al. Noble metal nanoparticles for biosensing applications. Sensors. 2012 Feb;12(2):1657–87.
[18] Vaseashta A, Vaclavikova M, Vaseashta S, Gallios G, Roy P, Pummakarnchana O. Nanostructures in environmental pollution detection, monitoring, and remediation. Sci Technol Adv Mater. 2007 Jan;8(1–2):47.
[19] Gadad AP, Kumar SV, Dandagi PM, Bolmol UB, Pallavi NP. Nanoparticles and their therapeutic applications in pharmacy. Int J Pharm Sci Nanotechnol. 2014 Aug;7(3):2515–6.
[20] Khandelwal A, Joshi R. Synthesis of nanoparticles and their application in agriculture. Acta Sci Agric. 2018;2(3):10–3.
[21] Matsui I. Nanoparticles for electronic device applications: a brief review. J Chem Eng Jpn. 2005;38(8):535–46.
[22] Stroyuk AL, Raevskaya AE, Kuchmiy SY, Dzhagan VM, Zahn DR, Schulze S. Structural and optical characterization of colloidal Se nanoparticles prepared via the acidic decomposition of sodium selenosulfate. Colloids Surf A: Physicochem Eng Asp. 2008 May;320(1–3):169–74.
[23] Lin W, Zhang J, Xu JF, Pi J. The advancing of selenium nanoparticles against infectious diseases. Front Pharmacology. 2021 Jul;12:682284.
[24] Maiyo F, Singh M. Selenium nanoparticles: Potential in cancer gene and drug delivery. Nanomedicine. 2017 May;12(9):1075–89.
[25] Mahmood RI, Abbass AK, Al-Saffar AZ, Al-Obaidi JR. An in vitro cytotoxicity of a novel pH-Sensitive lectin loaded-cockle shell-derived calcium carbonate nanoparticles against MCF-7 breast tumour cell. J Drug Delivery Sci Technol. 2021 Feb;61:102230.
[26] Soenen SJ, Rivera-Gil P, Montenegro JM, Parak WJ, De Smedt SC, Braeckmans K. Cellular toxicity of inorganic nanoparticles: common aspects and guidelines for improved nanotoxicity evaluation. Nano Today. 2011 Oct;6(5):446–65.
[27] Alam H, Khatoon N, Khan MA, Husain SA, Saravanan M, Sardar M. Synthesis of selenium nanoparticles using probiotic bacteria Lactobacillus acidophilus and their enhanced antimicrobial activity against resistant bacteria. J Clust Sci. 2020 Sep;31:1003–11.
[28] Husen A, Siddiqi KS. Plants and microbes assisted selenium nanoparticles: characterization and application. J Nanobiotechnology. 2014 Dec;12:1–10.
[29] Nada HG, Ali HE, El-Behery RR, Shanab SM, Elshatoury EH. Nanoparticles biosynthesized by bacillus cereus filtrate and gamma rays enhancing Chlorella vulgaris biomass and lipid production. J Clust Sci. 2022;33:2055–68.
[30] Chen W, Li X, Cheng H, Xia W. Chitosan-based selenium composites as potent Se supplements: Synthesis, beneficial health effects, and applications in food and agriculture. Trends Food Sci Technol. 2022 Nov 1;129:339–52.
[31] Memar MY, Adibkia K, Farajnia S, Kafil HS, Yekani M, Alizadeh N, et al. The grape seed extract: a natural antimicrobial agent against different pathogens. Rev Res Med Microbiology. 2019 Jul;30(3):173–82.
[32] Perumalla AV, Hettiarachchy NS. Green tea and grape seed extracts – Potential applications in food safety and quality. Food Res Int. 2011 May;44(4):827–39.
[33] Mahmoud YI. Grape seed extract neutralizes the effects of Cerastes cerastes cerastes post-synaptic neurotoxin in mouse diaphragm. Micron. 2013 Jan;44:298–302.
[34] Wadhwani SA, Shedbalkar UU, Singh R, Chopade BA. Biogenic selenium nanoparticles: current status and future prospects. Appl Microbiol Biotechnol. 2016 Mar;100:2555–66.
[35] Iranifam M, Fathinia M, Rad TS, Hanifehpour Y, Khataee AR, Joo SW. A novel selenium nanoparticles-enhanced chemiluminescence system for determination of dinitrobutylphenol. Talanta. 2013 Mar;107:263–9.
[36] Mahmood RI, Abbass AK, Razali N, Al-Saffar AZ, Al-Obaidi JR. Protein profile of MCF-7 breast cancer cell line treated with lectin delivered by CaCO3NPs revealed changes in molecular chaperones, cytoskeleton, and membrane-associated proteins. Int J Biol Macromol. 2021 Aug;184:636–47.
[37] Rahmah MI, Saadoon NM, Mohasen AJ, Kamel RI, Fayad TA, Ibrahim NM. Double hydrothermal synthesis of iron oxide/silver oxide nanocomposites with antibacterial activity. J Mech Behav Mater. 2021 Jan;30(1):207–12.
[38] Aziz WJ, Abid MA, Hussein EH. Biosynthesis of CuO nanoparticles and synergistic antibacterial activity using mint leaf extract. Mater Technol. 2020 Jul;35(8):447–51.
[39] Shahabadi N, Zendehcheshm S, Khademi F. Selenium nanoparticles: Synthesis, in-vitro cytotoxicity, antioxidant activity and interaction studies with ct-DNA and HSA, HHb and Cyt c serum proteins. Biotechnol Rep. 2021 Jun;30:e00615.
[40] Shar AH, Lakhan MN, Wang J, Ahmed M, Alali KT, Ahmed R, Ali I, et al. Facile synthesis and characterization of selenium nanoparticles by the hydrothermal approach. Dig J Nanomater Biostruct. 2019 Oct;14:867–72.
[41] Ramamurthy CH, Sampath KS, Arunkumar P, Kumar MS, Sujatha V, Premkumar K, et al. Green synthesis and characterization of selenium nanoparticles and its augmented cytotoxicity with doxorubicin on cancer cells. Bioprocess Biosyst Eng. 2013 Aug;36:1131–9.
[42] Jabir MS, Abood NA, Jawad MH, Öztürk K, Kadhim H, Albukhaty S, et al. Gold nanoparticles loaded TNF-α and CALNN peptide as a drug delivery system and promising therapeutic agent for breast cancer cells. Mater Technol. 2022 Dec;37(14):3152–66.
[43] Al-Rahim AM, Mahmood RI, Mohammed MM, Omer D. In vitro evaluation of antioxidant and cytotoxic activity of folate-methotrexate conjugated to bovine serum albumin nanoparticles against MCF-7, HepG2, and PC3 cell lines. Gene Rep. 2022 Dec;29:101666.

[44] Mohammed-Salih HS, Ghazi A, Mahmood RI, Al-Qazzaz HH, Supian FL, Al-Obaidi JR, et al. Enhancing orthodontic treatment control with fish scale-derived hydroxyapatite nanoparticles: Insights from an animal model study. Saudi Dental J. 2024 Aug;36(8):1128–34.
[45] Mohammed SA, Khashan KS, Jabir MS, Abdulameer FA, Sulaiman GM, Al-Omar MS, et al. Copper oxide nanoparticle-decorated carbon nanoparticle composite colloidal preparation through laser ablation for antimicrobial and antiproliferative actions against breast cancer cell line, MCF-7. BioMed Res Int. 2022;2022(1):9863616.
[46] Hadi NA, Mahmood RI, Al-Saffar AZ. Evaluation of antioxidant enzyme activity in doxorubicin treated breast cancer patients in Iraq: a molecular and cytotoxic study. Gene Rep. 2021 Sep;24:101285.
[47] Abbas ZS, Sulaiman GM, Jabir MS, Mohammed SA, Khan RA, Mohammed HA, et al. Galangin/β-cyclodextrin inclusion complex as a drug-delivery system for improved solubility and biocompatibility in breast cancer treatment. Molecules. 2022 Jul;27(14):4521.
[48] Farhana A, Lappin SL. Biochemistry, lactate dehydrogenase. InStatPearls [internet]. Treasure Island FL: StatPearls Publishing; 2023 May.
[49] Khashan KS, Jabir MS, Abdulameer FA. Carbon Nanoparticles decorated with cupric oxide Nanoparticles prepared by laser ablation in liquid as an antibacterial therapeutic agent. Mater Res Express. 2018 Mar;5(3):035003.
[50] Kazemi M, Akbari A, Soleimanpour S, Feizi N, Darroudi M. The role of green reducing agents in gelatin-based synthesis of colloidal selenium nanoparticles and investigation of their antimycobacterial and photocatalytic properties. J Clust Sci. 2019 May;30:767–5.
[51] Shakir M, Mohammed-Salih HS, Hussein FH, Al-Obaidi JR, Supian FL. Innovation of nano-hydrogels loaded with amelogenin peptide and hydroxyapatite nano-particles for remineralisation of artificially induced white spot lesions. J Drug Delivery Sci Technol. 2024 Sep;99:105986.
[52] Sengar M, Saxena S, Satsangee S, Jain R. Silver nanoparticles decorated functionalized multiwalled carbon nanotubes modified screen printed sensor for the voltammetric determination of butorphanol. J Appl Organomet Chem. 2021;1:95–108.
[53] Khosravanian A, Moslehipour A, Ashrafian H. A review on bioimaging, biosensing, and drug delivery systems based on graphene quantum dots. Prog Chem Biochem Res. 2021;4:44.
[54] Fernández-Llamosas H, Castro L, Blázquez ML, Díaz E, Carmona M. Speeding up bioproduction of selenium nanoparticles by using Vibrio natriegens as microbial factory. Sci Rep. 2017 Nov;7(1):16046.
[55] Srivastava N, Mukhopadhyay M. Biosynthesis and structural characterization of selenium nanoparticles using Gliocladium roseum. J Clust Sci. 2015 Sep;26:1473–82.
[56] Cremonini E, Zonaro E, Donini M, Lampis S, Boaretti M, Dusi S, et al. Biogenic selenium nanoparticles: characterization, antimicrobial activity and effects on human dendritic cells and fibroblasts. Microb Biotechnol. 2016 Nov;9(6):758–71.
[57] Sharma G, Sharma AR, Bhavesh R, Park J, Ganbold B, Nam JS, et al. Biomolecule-mediated synthesis of selenium nanoparticles using dried Vitis vinifera (raisin) extract. Molecules. 2014 Feb;19(3):2761–70.
[58] Dhanjal S, Cameotra SS. Aerobic biogenesis of selenium nanospheres by Bacillus cereus isolated from coalmine soil. Microb Cell Factories. 2010 Dec;9:1–11.
[59] Srivastava N, Mukhopadhyay M. Green synthesis and structural characterization of selenium nanoparticles and assessment of their antimicrobial property. Bioprocess Biosyst Eng. 2015 Sep;38:1723–30.
[60] Vekariya KK, Kaur J, Tikoo K. ERα signaling imparts chemotherapeutic selectivity to selenium nanoparticles in breast cancer. Nanomed: Nanotechnol Biol Med. 2012 Oct;8(7):1125–32.
[61] Zare B, Babaie S, Setayesh N, Shahverdi AR. Isolation and characterization of a fungus for extracellular synthesis of small selenium nanoparticles. Nanomed J. 2013 Oct;1(1):13–9.
[62] Samrot AV, Ram Singh SP, Deenadhayalan R, Rajesh VV, Padmanaban S, Radhakrishnan K. Nanoparticles, a double-edged sword with oxidant as well as antioxidant properties – A review. Oxygen. 2022 Nov;2(4):591–604.
[63] Varlamova EG, Goltyaev MV, Mal'tseva VN, Turovsky EA, Sarimov RM, Simakin AV, et al. Mechanisms of the cytotoxic effect of selenium nanoparticles in different human cancer cell lines. Int J Mol Sci. 2021 Jul;22(15):7798.
[64] Spyridopoulou K, Aindelis G, Pappa A, Chlichlia K. Anticancer activity of biogenic selenium nanoparticles: apoptotic and immunogenic cell death markers in colon cancer cells. Cancers. 2021 Oct;13(21):5335.
[65] Tian J, Wei X, Zhang W, Xu A. Effects of selenium nanoparticles combined with radiotherapy on lung cancer cells. Front Bioeng Biotechnol. 2020 Nov;8:598997.
[66] Shen KT, Chen MH, Chan HY, Jeng JH, Wang YJ. Inhibitory effects of chitooligosaccharides on tumor growth and metastasis. Food Chem Toxicol. 2009 Aug;47(8):1864–71.
[67] Ramadan MA, Sharaky M, Faid AH. Ionic gelation synthesis, characterization and cytotoxic evaluation of chitosan nanoparticles on different types of human cancer cell models. Egypt J Chem. 2022 Feb;65(2):153–9.
[68] Cinat D, Coppes RP, Barazzuol L. DNA damage-induced inflammatory microenvironment and adult stem cell response. Front Cell Dev Biol. 2021 Oct;9:729136.
[69] Bisht G, Rayamajhi S, Kc B, Paudel SN, Karna D, Shrestha BG. Synthesis, characterization, and study of *in vitro* cytotoxicity of ZnO-Fe_3O_4 magnetic composite nanoparticles in human breast cancer cell line (MDA-MB-231) and mouse fibroblast (NIH 3T3). Nanoscale Res Lett. 2016;11:537.
[70] Kessler A, Hedberg J, Blomberg E, Odnevall I. Reactive oxygen species formed by metal and metal oxide nanoparticles in physiological media – a review of reactions of importance to nanotoxicity and proposal for categorization. Nanomaterials. 2022 Jun;12(11):1922.
[71] Tan J, Xiang Y, Xiong Y, Zhang Y, Qiao B, Zhang H. Crebanine induces ROS-dependent apoptosis in human hepatocellular carcinoma cells via the AKT/FoxO3a signaling pathway. Front Pharmacology. 2023 Feb;14:1069093.
[72] Di Stefano A, Frosali S, Leonini A, Ettorre A, Priora R, Di Simplicio FC, et al. GSH depletion, protein S-glutathionylation and mitochondrial transmembrane potential hyperpolarization are early events in initiation of cell death induced by a mixture of isothiazolinones in HL60 cells. Biochim Biophys Acta (BBA)-Molecular Cell Res. 2006 Feb;1763(2):214–25.
[73] Lee SH, Choi BY, Kho AR, Jeong JH, Hong DK, Lee SH, et al. Protective effects of protocatechuic acid on seizure-induced neuronal death. Int J Mol Sci. 2018 Jan;19(1):187.
[74] Muhammad N, Usmani D, Tarique M, Naz H, Ashraf M, Raliya R, et al. The role of natural products and their multitargeted approach to treat solid cancer. Cells. 2022 Jul;11(14):2209.

[75] Nazam N, Jabir NR, Ahmad I, Alharthy SA, Khan MS, Ayub R, et al. Phenolic acids-mediated regulation of molecular targets in Ovarian Cancer: current understanding and future perspectives. Pharmaceuticals. 2023 Feb;16(2):274.
[76] Mishra RK, Ahmad A, Kumar A, Ali A, Jori C, Tabrez S, et al. Cortisone-loaded stearoyl ascorbic acid based nanostructured lipid carriers alleviate inflammatory changes in DSS-induced colitis. Biomater Adv. 2023 May;148:213383.
[77] Mehta SL, Kumari S, Mendelev N, Li PA. Selenium preserves mitochondrial function, stimulates mitochondrial biogenesis, and reduces infarct volume after focal cerebral ischemia. BMC Neurosci. 2012 Dec;13:1–12.
[78] Shultz SR, Wright DK, Zheng P, Stuchbery R, Liu SJ, Sashindranath M, et al. Sodium selenate reduces hyperphosphorylated tau and improves outcomes after traumatic brain injury. Brain. 2015 May;138(5):1297–313.
[79] Khan MR, Alafaleq NO, Ramu AK, Alhosaini K, Khan MS, Zughaibi TA, et al. Evaluation of biogenically synthesized MgO NPs anticancer activity against breast cancer cells. Saudi. J Biol Sci. 2024 Jan;31(1):103874.
[80] Alserihi RF, Mohammed MR, Kaleem M, Khan MI, Sechi M, Zughaibi TA, et al. Comparative efficacy of epigallocatechin gallate and its nano-formulation in prostate cancer 3D spheroids model. J King Saud Univ-Sci. 2023 May;35(4):102627.
[81] Wang H, He Y, Liu L, Tao W, Wang G, Sun W, et al. Prooxidation and cytotoxicity of selenium nanoparticles at nonlethal level in sprague-dawley rats and buffalo rat liver cells. Oxid Med Cell Longev. 2020;2020(1):7680276.
[82] Kondaparthi P, Flora SJ, Naqvi S. Selenium nanoparticles: An insight on its Pro-oxidant and antioxidant properties. Front Nanosci Nanotechnol. 2019 Dec;6(1):5.